Proceedings of the Eighteenth International Conference on
Civil, Structural and Environmental Engineering Computing
Edited by: P. Iványi, J. Kruis and B.H.V. Topping
Civil-Comp Conferences, Volume 10, Paper 7.4
Civil-Comp Press, Edinburgh, United Kingdom, 2025
ISSN: 2753-3239, doi: 10.4203/ccc.10.7.4

Stochastic Nonlinear SDOF Model and Probabilistic Fragility Assessment of Steel Plates Under Blast Loading

F. Pinna and F. Stochino

Department of Civil, Environmental Engineering and Architecture, University of Cagliari, Italy

Abstract

We present a reduced-order single-degree-of-freedom (SDOF) formulation that couples non-linear material behaviour with rate-dependent steel properties and explicit uncertainty propagation for steel plates subjected to blast over-pressure. The model is calibrated against experimental data and finite-element simulations, achieving < 5 % error on peak displacement while cutting computational time by four orders of magnitude. A Monte-Carlo framework (15,000 realizations) treats TNT mass as a log-normal variable and delivers fragility curves for slight, moderate and severe damage states. Results show that, for a 3 mm plate, the β-parameter of the fitted sigmoid increases from 5.1 to 8.4 when explosive mass rises from 50 kg to 200 kg, indicating steeper reliability gradients. The proposed approach enables rapid performance-based assessment and is readily extendable to other impulsive loads or parameterized digital-twin environments.

Keywords: single-degree-of-freedom, stochastics, uncertain loading, Monte Carlo simulations, fragility curves, blast loading, steel plates.

1 Introduction

Structural elements, how plates, are exposed to blast loads, forces that rise and fall in milliseconds and vary across the surface. The peak pressure, duration and impulse are usually known only within wide uncertainty ranges. In settings such as industrial plants or dense city centers, safe design therefore needs two ingredients: a mechanical model that captures the plate's non-linear behavior to extreme loading, and a

probabilistic framework that carries all key uncertainties through to clear performance measures.

Recent experimental campaigns on metallic panels [1–3] have considerably improved the physical understanding of blast–structure interaction; yet their direct use in routine design remains limited because full three-dimensional non-linear finite-element (FE) analyses are computationally prohibitive when thousands of load/performance realizations are required.

A popular compromise is to replace the full continuum description with a reduced-order single-degree-of-freedom (SDOF) in which the plate is idealized as a lumped-mass, bilinear oscillator calibrated to replicate the dominant deformation mode [4-6]. Classical SDOF schemes, however, are mostly deterministic and linear-elastic; they neglect strain-rate effects and cannot be deployed in a Monte-Carlo environment without ad-hoc empirical corrections. Moreover, published fragility studies on extreme-loaded element often rely on simplified pressure–impulse diagrams or on machine-learning surrogates trained for seismic rather than impulsive demands [7-10]. Motivated by these gaps, the present work proposed a non-linear, strain-rate dependent SDOF formulation expressly devised for large-scale uncertainty propagation.

The remainder of the paper is organized as follows. Section 2 details the theoretical derivation of the SDOF, including load and mass factors, strain-rate modelling and the explicit central-difference integration scheme. Section 2.1 benchmarks the model against experimental and FEM results from the literature. Section 3 develops the probabilistic framework and the resulting fragility curves. Concluding remarks and avenues for future research are given in Section 4.

2 Methods

As illustrated in Figure 1, the steel plate is represented by a single-degree-of-freedom, SDOF, model with a resistance $R_{E,el/pl} = \alpha_{el/pl} \cdot M_R$, lumped mass, M_E, and stiffness, K_E, are taken from [6] for clamped square plates and simple support plates. The governing equations are:

$$M_{E,el}\frac{d^2U_E(t)}{dt^2} + K_{E,el}\,U_E(t) = F_E(t) \quad \text{for } 0 \le U_E \le U_{E,el} \tag{1a}$$

$$M_{E,pl}\frac{d^2U_E(t)}{dt^2} + K_{E,pl}\,U_E(t) = F_E(t) \quad \text{for } U_{E,el} < U_E \le U_{E,pl} \tag{1b}$$

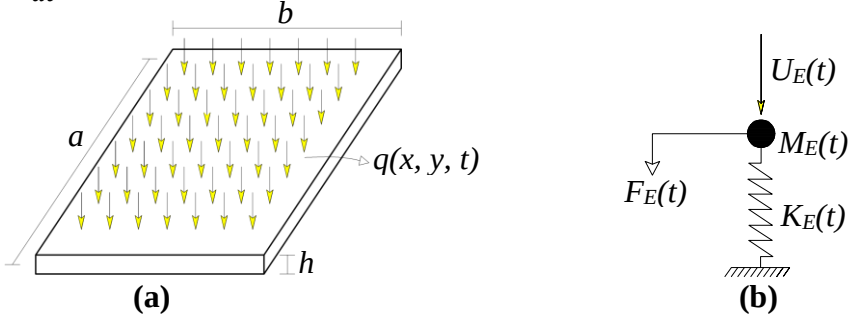

Figure 1: (a) Real plate; (b) SDOF model for the steel plate.

The equivalent load F_E is given by:

$$F_E(t) = K_L\, P_{max} \left(1 - \frac{t}{t_p}\right) a\, b \quad \text{for } 0 \le t \le t_p \tag{2a}$$

$$F_E(t) = 0 \quad \text{for } t_p < t \tag{2b}$$

Where P_{max}, is the maximum pressure of the explosion, t is the duration of the simulation, and t_p is the duration of the positive phase of the load. It should be noted that the equivalent load and stiffness are obtained by multiplying the force and the stiffness by the load factors (K_L) [6].

Blast loading subjects steel plates to strain rates that can exceed 10^2 s^{-1}[1]. Ignoring this effect would underestimate the dynamic yield stress and, hence, the overall resistance. In the present SDOF formulation the rate sensitivity of steel is introduced through the Cowper-Symonds law [11]:

$$f_{ykd}(t) = f_{yk}\left[1 + \left(\frac{\dot{\varepsilon}(t)}{D}\right)^{\frac{1}{q}}\right] \tag{3}$$

Where f_{yk} is the quasi-static yield strength, $\dot{\varepsilon}(t)$ is the instantaneous strain rate, and D and q are material constant (D = 40 s^{-1}, q = 5. How demonstrated in [12]). The rate-dependent model captures the elastic-plastic transition governed by a bilinear force-displacement relation, the amplification of yield strength given by Eq. (3), and the progressive change of boundary conditions that occurs when plastic hinges form along the plate edges (shown in Fig.2).

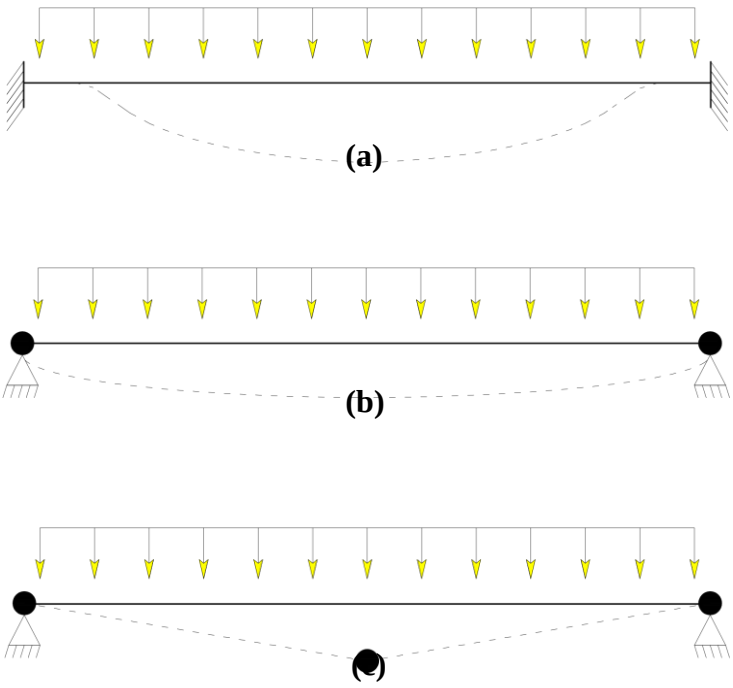

Figure 2: (a) Elastic phase; (b) Elastic-plastic phase; (c) Plastic phase.

For the elastic phase, $0 \le U_E \le U_{E,el}$, the equation of motion reads:

$$M_{E,el}\frac{d^2}{dt^2}\left(2\frac{a^2}{h}\frac{\alpha_{E,el}}{\beta_{E,el}}\frac{f_{ykd}(t)}{E}\right)+K_{E,el}\,2\frac{a^2}{h}\frac{f_{ykd}(t)}{E}\frac{\alpha_{E,el}}{\beta_{E,el}}=F_E(t) \tag{3a}$$

Where $M_{E,el}$ and $K_{E,el}$ are the elastic lumped mass and stiffness, a and h are plate half-span and thickness, and α and β are coefficient achieved by [6]. Once the mid-span displacement exceeds the elastic limit, $U_{E,el} < U_E \le U_{E,pl}$, the tangent stiffness changes to $K_{E,pl}$ and Eq. (3a) become:

$$\begin{aligned} &M_{E,pl}\frac{d^2}{dt^2}\left(2\frac{a^2}{h}\frac{f_{ykd}(t)}{E}\left[\frac{\alpha_{E,el}}{\beta_{E,el}}+\left(\frac{\alpha_{E,pl}-\alpha_{E,el}}{\beta_{E,pl}}\right)\right]\right)+ \\ &K_{E,pl}\left(2\frac{a^2}{h}\frac{f_{ykd}(t)}{E}\left[\frac{\alpha_{E,el}}{\beta_{E,el}}+\left(\frac{\alpha_{E,pl}-\alpha_{E,el}}{\beta_{E,pl}}\right)\right]\right)=F_E(t) \end{aligned} \tag{3b}$$

Where subscripts pl denote fully plastic values. At any plate point, (x, y), the transverse displacement, w, is expressed as the product of an SDOF generalized coordinate, $Y(t)$, and a spatial mode shape, $\Psi(x, y)$:

$$w(x,y,t)=Y(t)\Psi(x,y) \tag{4}$$

For clamped edges:

$$\Psi(w,y)=cos^2\left(\frac{\pi}{a}x\right)cos^2\left(\frac{\pi}{b}y\right) \tag{5a}$$

$$w(x,y,t)=Y(t)cos^2\left(\frac{\pi}{a}x\right)cos^2\left(\frac{\pi}{b}y\right) \tag{5b}$$

For simply supported edges:

$$\Psi(w,y)=cos\left(\frac{\pi}{a}x\right)cos\left(\frac{\pi}{b}y\right) \tag{6a}$$

$$w(x,y,t)=Y(t)cos\left(\frac{\pi}{a}x\right)cos\left(\frac{\pi}{b}y\right) \tag{6b}$$

As described by [13] the curvatures are equal to the second time derivatives of displacements. For the case of fixed along all edges are:

$$\frac{\partial^2 w(x,y,t)}{\partial x^2}=-2Y(t)\left(\frac{\pi}{a}\right)^2\left[cos^2\left(\frac{\pi}{a}x\right)-sin^2\left(\frac{\pi}{a}x\right)\right]cos^2\left(\frac{\pi}{b}y\right) \tag{7a}$$

And the corresponding curvature-rate is:

$$\dot{\theta}_x(x,y,t)=-2\dot{Y}(t)\left(\frac{\pi}{a}\right)^2\left[cos^2\left(\frac{\pi}{a}x\right)-sin^2\left(\frac{\pi}{a}x\right)\right]cos^2\left(\frac{\pi}{b}y\right) \tag{7b}$$

And for the phase with simple support on all edges:

$$\frac{\partial^2 w(x,y,t)}{\partial x^2}=\theta_x(x,y,t)=-Y(t)\left(\frac{\pi}{a}\right)^2 cos\left(\frac{\pi}{a}x\right)cos\left(\frac{\pi}{b}y\right) \tag{8a}$$

$$\dot{\theta}_x(x,y,t) = -\dot{Y}(t)\left(\frac{\pi}{a}\right)^2 cos\left(\frac{\pi}{a}x\right) cos\left(\frac{\pi}{b}y\right) \quad (8b)$$

At every time step, $\dot{\theta}_x$ provides the instantaneous strain-rate, which is substituted back into Eq. (3) to update the dynamic yield strength and, in turn, the resistance terms in Eq. (3). This algorithm ensures full coupling between material-rate effects and global plate kinematics.

3 Validation

Validation of SDOF model is carried out on real-experimental data obtained from [1] and a companion finite-element (FE) model of a square plate (610 mm x 610 mm x 12.7 mm) subjected to a 1 kg TNT charge at a 146 mm stand-off distance. The test rig, reproduced from [1], is sketched in Figure 3; Figure 4 shows the FE contour plot of the out-of-plane displacement at the instant of peak response.

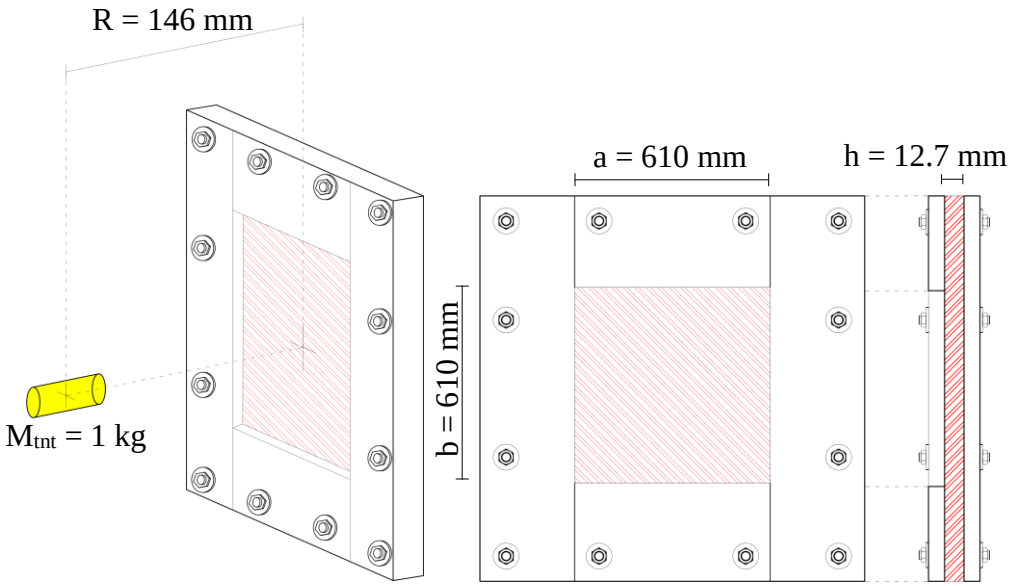

Figure 3: Experimental apparatus used in [1].

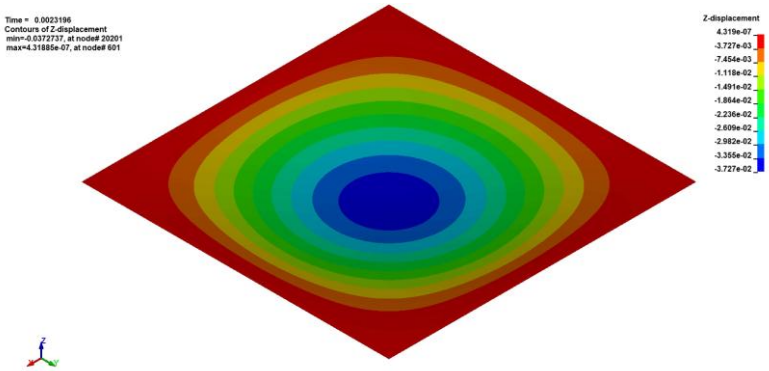

Figure 4: FE contour plot of the out-of-plane displacement at the instant of peak pressure.

The proposed SDOF predicts the mid-span time history with a peak-error of 4.7 % relative to the experimental trace (shown in Figure 5). It also matches the FEM envelope while suppressing the high-frequency flexural content that is outside the single-mode assumption.

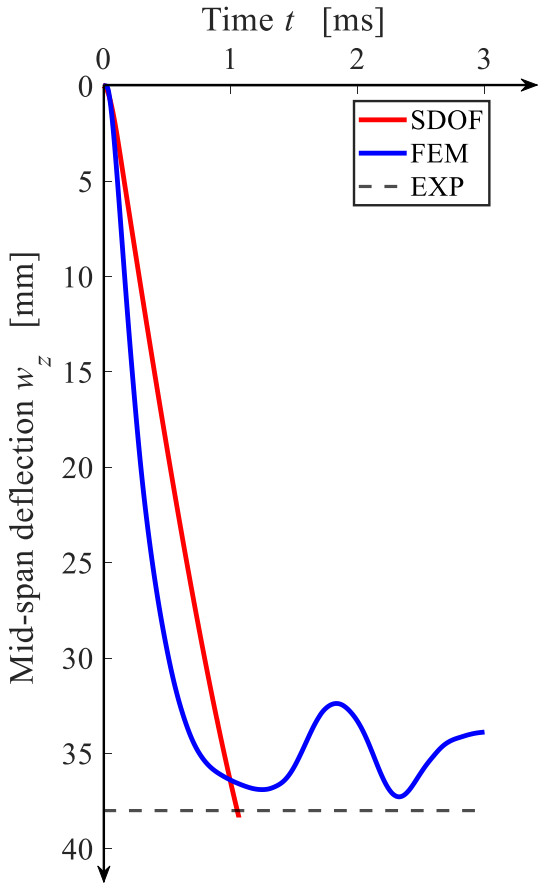

Figure 5: Measured versus modelled mid-span deflection history: experiment (dashed), FE (blue), SDOF (red).

The computational cost is reduced by four orders of magnitude: an identical (Intel Core i7-11800H processor, 16 GB DDR4 RAM, 1024 GB SSD) full FEM results require 12 min, whereas the SDOF solution is obtained in 0.01 s. The agreement demonstrates that the reduced-order formulation retains sufficient fidelity for blast assessments while enabling the large number of realizations required for the probabilistic study presented in Section 4.

4 Results

Leveraging the computational speed of the SDOF, 15,000.00-run Monte-Carlo simulations were performed to derive fragility curves for three damage states-slight, moderate and severe-as a function of Hopkinson-scaled distance Z [14]. TNT charge mass, M_{TNT}, was treated as a log-normal variable; the base case considers μ = 50, 100 and 200 kg with a coefficient of variation of 10 %. The peak reflected pressure applied in each realization follows the Kinney and Graham correlation [15].

$$P_{max} = P_0 \frac{808\left[1+\left(\frac{Z}{4.5}\right)^2\right]}{\sqrt{\left[1+\left(\frac{Z}{0.0408}\right)^2\right]\left[1+\left(\frac{Z}{0.32}\right)^2\right]\left[1+\left(\frac{Z}{1.35}\right)^2\right]}} \quad (9)$$

Where $\boldsymbol{P_0}$ is the initial pressure. Performance levels are defined directly from the SDOF displacement response, is shown in Table 1.

Table 1: Displacements thresholds for performance levels, extracted from SDOF.

Slight Damage	Moderate Damage	Severe Damage
$U_{E,el}$	$U_{E,pl} = U_{E,el} + \frac{U_{E,pl} - U_{E,el}}{2}$	$U_{E,pl}$

The exceedance probability for a generic response variable, X, is obtained by numerical convolution:

$$P(X > x_o) = \int_{-\infty}^{+\infty} P(X > x_0|Z)p(Z)dz \cong \sum_{i=0}^{\infty} P(X > x_0|Z)_i \, p(Z)_i \Delta Z_i \quad (10)$$

The discrete exceedance points are approximated with a two-parameter sigmoid:

$$f(Z,\beta) = \frac{1}{1 + exp^{-b_1(Z-b_2)}} \quad (11)$$

$f(Z,\beta)$ is the sigmoid function representing the probability of exceeding the specified damage threshold at a given scaled distance Z. The output ranges between 0 and 1, capturing the cumulative probability of exceeding failure as the distance changes. β is a vector containing the parameters of the sigmoid function, which are estimated during the nonlinear regression fitting process. Specifically: b_1 controls the slope of the sigmoid curve and b_2 modifies the position of the inflection point of the sigmoid. The parameters b_1 and b_2 are estimated using a nonlinear regression fitting process, which iteratively modify these values to minimize the difference between the observed probabilities from the Monte Carlo analysis and those predicted by the sigmoid function. To ensure the reliability of the analysis, a target coefficient of variation (COV) below 10% was set for the maximum displacements [16]. The COV represents the ratio of the standard deviation to the mean, providing a normalized measure of the variability in the data relative to the average value. However, in cases where this target could not be achieved within 15,000.00 iterations, the analysis was terminated to avoid excessive computation times [7-10]. We recall that the computations were performed on a notebook with an Intel Core i7-11800H processor, 16 GB DDR4 RAM, 1024 GB SSD. On average, each curve requires approximately 18 hours of computation time. The analysis was performed on a sample plate whose properties are shown in Table 2.

Table 2: Properties of sample plate for fragility curves.

Properties of sample solid steel plate for fragility curves	
Length a	0.700 m
Width b	0.700 m
Thickness h	0.003 m
Density ρ	7850 kg/m^3
Steel yield strength f_{yk}	275 MPa
Steel elastic modulus E	210 GPa
Positive phase time t_p	1 ms

The fragility curves for the experimental plates, shown in Figures 6-8, were produced considering the following TNT mass as a lognormal distribution with mean values of 50, 100 and 200 kg.

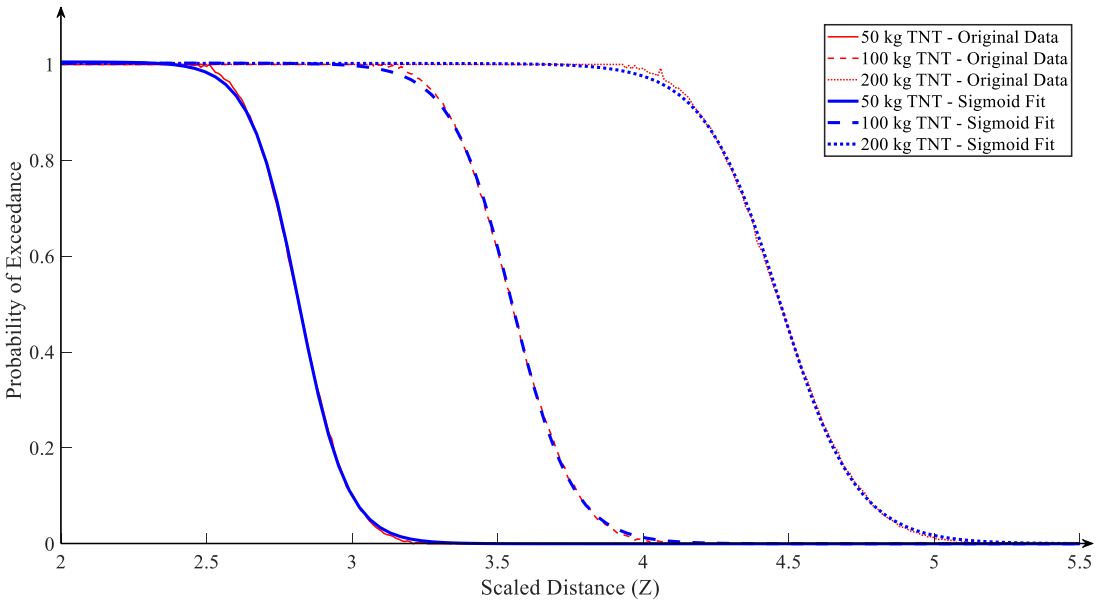

Figure 6: Fragility curves slight damage conditions for the steel plate shown in Table 2.

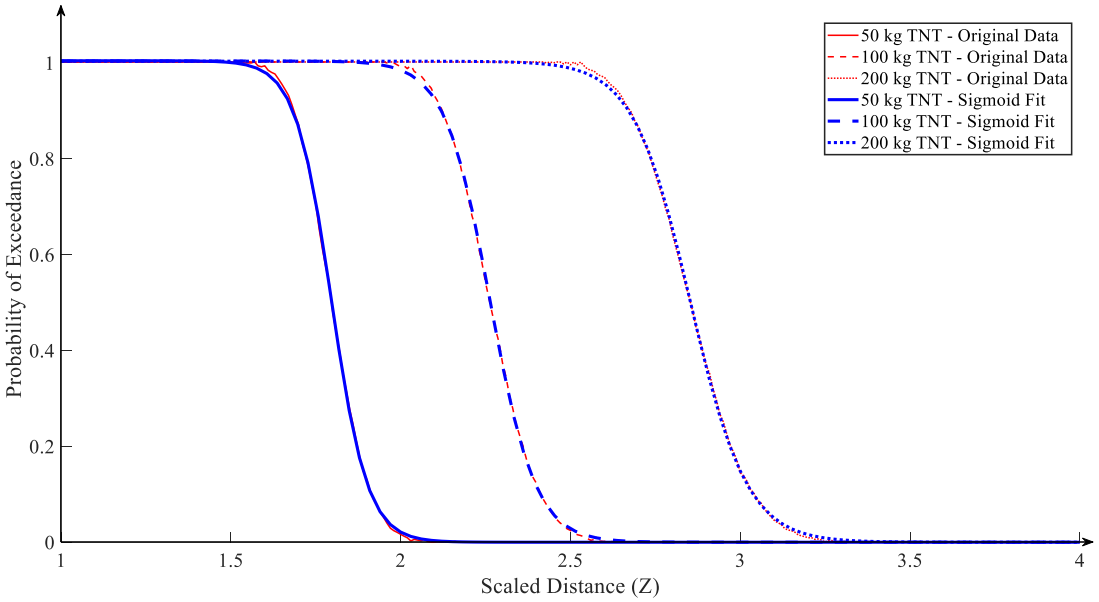

Figure 7: Fragility curves moderate damage conditions for the steel plate shown in Table 2.

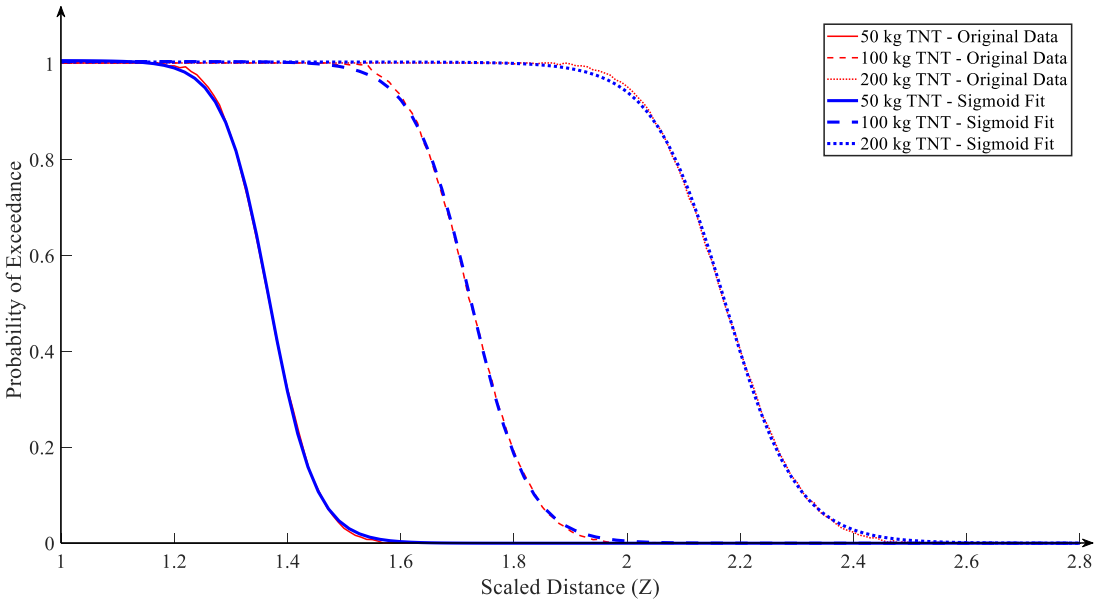

Figure 8: Fragility curves severe damage conditions for the steel plate shown in Table 2.

5 Conclusions

A rate-dependent, bilinear single-degree-of-freedom (SDOF) model has been developed and validated as a rapid alternative to full non-linear-element (FE) analysis for blast-loaded steel plates. The model reproduces peak mid-span displacement within 5 % experimental data while cutting CPU time from minutes to milliseconds, making large-scale Monte-Carlo studies feasible on a standard laptop.

By embedding the SDOF in a 15,000.00-run probabilistic framework, fragility curves were produced for slight, moderate and severe damage states and for TNT masses of 50-200 kg. Results show that the median capacity distance increases and the slope b_1 steepens with charge mass, and the transition between damage states narrows as deformation enters the plastic range.

The curves provide designers with a computationally inexpensive, yet mechanically grounded tool for performance-based blast assessment and for screening mitigation options in the early stages of the project. Because the model is reduced order, its accuracy depends on correct calibration of elastic and plastic stiffness parameters; application to real structures should therefore be preceded by benchmarking against test data or high-fidelity simulations.

Future work extends the formulation to other impulsive actions such as local impact or debris strikes, couple the SDOF with surrogate-based global-sensitivity analysis to quantify parameter importance, and integrate the approach into a digital-twin framework for real-time reliability updating. Comparative studies with advanced FEM-based stochastic methods are planned to further delineate the range of validity and computational advantages of the proposed model.

References

[1] Dharmasena, K. P., Wadley, H. N., Xue, Z., & Hutchinson, J. W. (2008). *Mechanical response of metallic honeycomb sandwich panel structures to high-intensity dynamic loading*. International Journal of Impact Engineering, 35(9), 1063-1074. https://doi.org/10.1016/j.ijimpeng.2007.06.008

[2] Wang, Y., Li, W., Zhu, W., Zhang, Q., Li, W., & Wang, X. (2024). *Dynamic response of steel cabin structure under blast loading from adjacent cabin*. Engineering Structures, 311, 118213. https://doi.org/10.1016/j.engstruct.2024.118213

[3] Zheng, C., Kong, X. S., Wu, W. G., Xu, S. X., & Guan, Z. W. (2018). *Experimental and numerical studies on the dynamic response of steel plates subjected to confined blast loading*. International Journal of Impact Engineering, 113, 144-160. https://doi.org/10.1016/j.ijimpeng.2017.11.013

[4] Mays, G., & Smith, P. D. (Eds.). (1995). *Blast effects on buildings: Design of buildings to optimize resistance to blast loading*. Thomas Telford.

[5] DoD, U. S. (2008). *Structures to resist the effects of accidental explosions*. Unified Facilities Criteria, United States of America, Department of Defense, Washington, DC, Document No. UFC, 3-340.

[6] Biggs, J. M. (1964). *Introduction to structural dynamics*.

[7] Olmati, P., Petrini, F., & Gkoumas, K. (2014). *Fragility analysis for the Performance-Based Design of cladding wall panels subjected to blast load*. Engineering Structures, 78, 112-120. https://doi.org/10.1016/j.engstruct.2014.06.004

[8] Kiani, J., Camp, C., & Pezeshk, S. (2019). *On the application of machine learning techniques to derive seismic fragility curves*. Computers & Structures, 218, 108-122. https://doi.org/10.1016/j.compstruc.2019.03.004

[9] Seo, J., Hatlestad, A. J., Kimn, J. H., & Hu, J. W. (2022). *Application of mathematical functions for seismic increment fragility determination*. European Journal of Environmental and Civil Engineering, 26(2), 473-480. https://doi.org/10.1080/19648189.2019.1665106

[10] Li, Z., Wu, Z., Lu, X., Zhou, J., Chen, J., Liu, L., & Pei, L. (2022). *Efficient seismic risk analysis of gravity dams via screening of intensity measures and simulated non-parametric fragility curves*. Soil Dynamics and Earthquake Engineering, 152, 107040. https://doi.org/10.1016/j.soildyn.2021.107040

[11] Cowper, G. R., & Symonds, P. S. (1957). *Strain hardening and strain rate affect the impact loading of cantilever beams*. Brown University. Division of Applied Mathematics report, 28.

[12] Carta, G., & Stochino, F. (2013). *Theoretical models to predict the flexural failure of reinforced concrete beams under blast loads*. Engineering structures, 49, 306-315. https://doi.org/10.1016/j.engstruct.2012.11.008

[13] Timoshenko, S. (1959). Theory of Plates and Shells.

[14] Hopkinson, B. (1914). X. *A method of measuring the pressure produced in the detonation of high, explosives or by the impact of bullets*. Philosophical Transactions of the Royal Society of London. Series A, Containing Papers of a Mathematical or Physical Character, 213(497-508), 437-456. https://doi.org/10.1098/rsta.1914.0010

[15] Kinney, G. F., & Graham, K. J. (2013). *Explosive shocks in air*. Springer Science & Business Media.

[16] Stochino, F., Attoli, A., & Concu, G. (2020). *Fragility curves for RC structure under blast load considering the influence of seismic demand*. Applied Sciences, 10(2), 445. https://doi.org/10.3390/app10020445